Fair and Efficient Profit Allocation for Collaborative Operation of Distributed Renewable Energy Operators and Electric Vehicle Charging Stations

Wei Zha, Haiwang Zhong, *Senior Member*, *IEEE*, and Yinyan Liu, *Member*, *IEEE*

***Abstract*—The difficulty in capital recovery for distributed renewable energy operators (DREOs) and the high charging costs at electric vehicle charging stations (EVCSs) have long been significant challenges in power systems. Collaborative operation of DREOs and EVCSs can effectively address these challenges, yet few studies have approached incentivizing collaboration from the perspective of profit allocation. Therefore, this paper proposes a fair and efficient profit allocation method. Incorporating the Gauss-Legendre quadrature formula into the Aumann-Shapley value (GL-AS) method enables efficient calculation of the profit allocation of cooperative members. However, existing literature only discusses the profit allocation method of conventional power generation units, limiting its applicability. This paper addresses the problem of energy storage system (ESS) switching between charging and discharging in any time interval and the time-varying problem of renewable energy power output, thereby ensuring the efficiency of the solution process. Furthermore, a novel profit allocation adjustment model is provided through the adoption of triangular fuzzy comprehensive evaluation (TFCE). Finally, the effectiveness of the proposed profit allocation method is validated through numerical simulations in various scenarios.**

***Index Terms*—Electric vehicle charging station, distributed renewable energy operator, profit allocation, Aumann-Shapley value, analytic hierarchy process, entropy weight.**

I. Introduction

In recent years, the installed capacity of renewable energy has significantly increased on a global scale. It is projected that by 2030, the installed capacity of wind power (WP) and photovoltaic (PV) in China will reach 1200 GW, with the majority existing in a distributed form [1]. However, distributed renewable energy generation faces challenges related to profitability and extended periods for capital recovery [2], [3]. Concurrently, electric vehicles (EVs), as a new generation of transportation electrification tools, are being widely adopted, yet the high electricity purchasing costs for electric vehicle charging stations (EVCSs) contribute to their elevated operational expenses [4], [5]. Reducing the operational costs of EVCSs is a critical issue that needs to be addressed in the context of transportation electrification.

Collaborative operations between distributed renewable energy operators (DREOs) and EVCSs can effectively solve their profitability issues. DREOs can supply EVs with clean energy for charging, thereby providing cheaper power for EVCSs. Meanwhile, DREOs also avoid selling power to system operator (SO) at relatively low prices [6], [7]. Currently, some studies have explored the collaborative operations of DREOs and EVCSs. Planning for the optimal scale and siting of distributed renewable energy and EVs, which reduces the costs of collaborative operation, has been discussed in [8], [9]. The economics of collaborative operation between multiple types of EVs and distributed PV systems have been evaluated in [10]. However, few studies have been conducted from the perspective of profit allocation to motivate the cooperation between DREOs and EVCSs.

Addressing profit allocation problems is crucial as it impacts the fairness and stability of cooperative alliances, ensuring that each cooperative member is adequately compensated for their contributions, thereby fostering sustainable long-term cooperation. The existing profit allocation methods mainly include the Nash bargaining theory, Vickrey-Clarke-Groves (VCG) mechanism, and Shapley value method. The Nash bargaining theory is used to allocate the profits from the cooperative operation of integrated energy systems [11], [12]. However, the disagreement point in Nash bargaining theory is difficult to determine in practice [13], and the complexity of the model significantly increases as the number of cooperating members grows. The VCG mechanism is used to allocate profits among market participants cooperating in the energy market, ancillary service market,

Manuscript received: May 22, 2024; revised: August 30, 2024; accepted: October 19, 2024. Date of CrossCheck: October 19, 2024. Date of online publication: November 15, 2024.

This work was supported in part by the National Natural Science Foundation of China (No. 52122706) and in part by the Tsinghua University Initiative Scientific Research Program.

W. Zha and H. Zhong (corresponding author) are with the State Key Laboratory of Power System Operation and Control, Department of Electrical Engineering, Tsinghua University, Beijing 100084, China, and they are also with Sichuan Energy Internet Research Institute, Tsinghua University, Beijing 100190, China (e-mail: zhaw22@mails.tsinghua.edu.cn; zhonghw@tsinghua.edu.cn).

Y. Liu is with the School of Photovoltaic and Renewable Energy Engineering, University of New South Wales, Sydney, Australia (e-mail: yinyan. yana. liu@gmail.com).

DOI: 10.35833/MPCE.2024.000534

and carbon market. While the allocation results satisfy incentive compatibility [14], [15], they do not meet the budget balance condition [16], [17]. The Shapley value method is the only allocation method that satisfies a series of axioms such as efficiency, fairness, and symmetry. It is applicable to any cooperative game and can be used in various fields such as cost-sharing, profit allocation, and resource allocation. However, it is observed that the computation time for the Shapley value method increases exponentially with the number of cooperative members. As an improvement over the Shapley value method, the Aumann-Shapley value (AS) method has been effectively employed to enhance computational speed and has been widely adopted in the field of power systems [18], [19]. The participation of ESSs in the carbon emission allocation market is analyzed using the AS method in [20], but the problem of ESS charging and discharging switching in any time interval is not discussed. Similarly, the Gauss-Legendre quadrature formula into the Aumann-Shapley value (GL-AS) method is proposed to achieve efficient resolution of profit allocation problems within cooperative alliances in [21], yet it only discusses the profit allocation of conventional power generation units. The profit allocation method that is widely applicable to various resources in power systems while balancing fairness and efficiency has not yet been proposed.

Furthermore, as an evolution of the Shapley value method, the GL-AS method also inherits the limitations of assigning equal status to all cooperative members without considering the responsibility and the factors affecting cooperation. Improvements to the Shapley value method have been attempted by introducing risk factors, cost factors, and contribution factors [22], [23], yet these modifications fail to address the problem of weight allocation among various factors and fail to take into account the subjective opinions of cooperative members. The triangular fuzzy comprehensive evaluation (TFCE) method, integrating the subjective assessment of the analytic hierarchy process with triangular fuzzy numbers (TFN-AHP) and the objective assessment of the entropy weight (EW), has been demonstrated to effectively handle the uncertainty and fuzziness of multiple evaluation indicators, thereby enhancing the accuracy of weight distribution among indicators. This method has been extensively applied in solving problems related to risk assessment [24], [25], performance evaluation [26], decision-making assessment [27], etc. Yet, the TFCE method has not been applied to the profit allocation adjustment model under the multi-factor situation of the GL-AS method.

In summary, given the scarcity of research on the collaborative operation and profit allocation between DREOs and EVCSs, as well as the imperfections in existing methods, an fair and efficient profit allocation method is proposed in this paper. In the process of profit allocation, all cooperative members must adhere to the cooperative alliance agreement, working together to ensure that the cooperative alliance achieves the maximum profit. Using scenario generation methods, typical output scenarios of WP and PV are generated. Since the power outputs of WP and PV vary across each time interval, progressively analyzing each time interval can effectively address the time-varying problem in the power output of DREOs. Due to the potential for ESSs to charge or discharge in any time interval, employing the GL-AS method and AS method for direct resolution presents considerable difficulties. The Big-M method is introduced to address these difficulties. In the process of collaborative operation between EVCSs and DREOs, the risk level (RL), profit contribution rate (PCR), and profit growth rate (PGR) are considered as factors influencing profit allocation. Finally, the TFCE method is used to conduct both subjective and objective assessments of the wights of these factors, thereby achieving fairness in profit allocation. The main contributions of this paper are threefold.

1) The collaborative and independent operation models are established for DREOs and EVCSs, with the DREOs including distributed WP and PV. The charging models in EVCSs are primarily composed of smart charging (SC) model and vehicle-to-grid (V2G) model.

2) A detailed solution method for the profit allocation between EVCSs and DREOs based on the GL-AS method is proposed. The profit allocation solution speed is nearly ten times faster than the AS method, which is adaptable to various resources within the power system.

3) By employing the TFCE method, subjective and objective assessments are conducted on various factors including RL, PGR, and PCR, thereby achieving fairness in profit allocation.

The specific structure of this paper is as follows. The DREO and EVCS models are formulated in Section II. The independent and collaborative operation models are presented in Section III. The proposed profit allocation method is discussed in Section IV. The profit allocation adjustment model is presented in Section V. Section VI presents case studies and simulation results. Finally, Section VII concludes this paper.

II. Model Formulation

A. General Description

As depicted in Fig. 1, the collaborative operation model established in this paper is primarily composed of three entities: DREOs, EVCSs, and SO. DREOs are equipped with ESSs. In EVCSs, EV owners have the option to select from two charging models, i.e., SC and V2G.

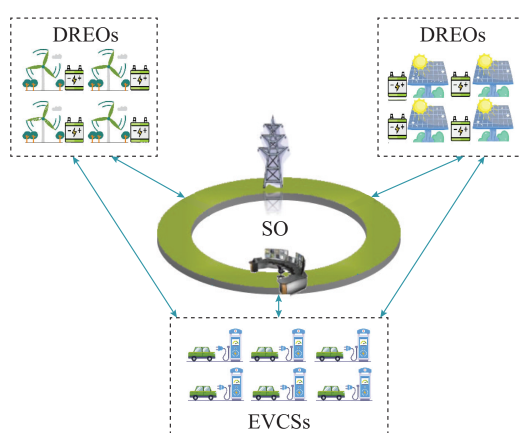

Fig. 1. Collaborative operation model.

When operating independently, DREOs are constrained to sell their generated power to SO at relatively low prices. When operating independently, EVCSs are compelled to purchase power from SO at relatively high prices. However, when DREOs and EVCSs engage in collaborative operation, DREOs can sell power to SO while also providing power to EVCSs. EVCSs can directly utilize the power provided by DREOs, thereby reducing operational costs and achieving a win-win situation.

B. Typical Scenario Generation Methods

Copula theory is frequently employed in scenario generation by decomposing the joint distribution function into marginal distribution functions and a Copula function, thereby investigating the randomness and correlation among variables and simplifying the computation of joint distributions [28]. From the scenario set generated using Copula theory, S typical scenarios are then selected through the application of the K-means method [29].

C. Arrival and Departure Charging Time for EV Owners

Based on the charging requirements of EV owners, EV charging is generally categorized into two patterns: residential charging and public charging.

In the public charging pattern, EV owners initiate charging upon arrival at their workplace and conclude charging upon completion of their work. The distribution functions of EV arrival time t_p^a and departure time t_p^d are given in (1) and (2), respectively.

$$f\left(t_p^a\right)=\begin{cases}\dfrac{1}{\sqrt{2\pi}\,\sigma_{p_a}}\exp\left(-\dfrac{\left(t_p^a+24-\mu_{p_a}\right)^2}{2\sigma_{p_a}^2}\right) & 0<t_p^a\leq\mu_{p_a}-12\\ \dfrac{1}{\sqrt{2\pi}\,\sigma_{p_a}}\exp\left(-\dfrac{\left(t_p^a-\mu_{p_a}\right)^2}{2\sigma_{p_a}^2}\right) & \mu_{p_a}-12<t_p^a\leq 24\end{cases} \tag{1}$$

$$f\left(t_p^d\right)=\begin{cases}\dfrac{1}{\sqrt{2\pi}\,\sigma_{p_d}}\exp\left(-\dfrac{\left(t_p^d+24-\mu_{p_d}\right)^2}{2\sigma_{p_d}^2}\right) & 0<t_p^d\leq\mu_{p_d}+12\\ \dfrac{1}{\sqrt{2\pi}\,\sigma_{p_d}}\exp\left(-\dfrac{\left(t_p^d-\mu_{p_d}\right)^2}{2\sigma_{p_d}^2}\right) & \mu_{p_d}+12<t_p^d\leq 24\end{cases} \tag{2}$$

where μ_{p_a} and σ_{p_a} are the normal distribution parameters of EV arrival time in the public charging pattern; μ_{p_d} and σ_{p_d} are the normal distribution parameters of EV departure time in the public charging pattern; and $f(\cdot)$ is the distribution function.

In the residential pattern, EV owners initiate charging upon returning their home and conclude charging upon departure. The distribution functions of EV arrival time t_h^a and departure time t_h^d can be shown as in (3) and (4), respectively.

$$f\left(t_h^a\right)=\begin{cases}\dfrac{1}{\sqrt{2\pi}\,\sigma_{h_a}}\exp\left(-\dfrac{\left(t_h^a+24-\mu_{h_a}\right)^2}{2\sigma_{h_a}^2}\right) & 0<t_h^a\leq\mu_{h_a}+12\\ \dfrac{1}{\sqrt{2\pi}\,\sigma_{h_a}}\exp\left(-\dfrac{\left(t_h^a-\mu_{h_a}\right)^2}{2\sigma_{h_a}^2}\right) & \mu_{h_a}+12<t_h^a\leq 24\end{cases} \tag{3}$$

$$f\left(t_h^d\right)=\begin{cases}\dfrac{1}{\sqrt{2\pi}\,\sigma_{h_d}}\exp\left(-\dfrac{\left(t_h^d+24-\mu_{h_d}\right)^2}{2\sigma_{h_d}^2}\right) & 0<t_h^d\leq\mu_{h_d}-12\\ \dfrac{1}{\sqrt{2\pi}\,\sigma_{h_d}}\exp\left(-\dfrac{\left(t_h^d-\mu_{h_d}\right)^2}{2\sigma_{h_d}^2}\right) & \mu_{h_d}-12<t_h^d\leq 24\end{cases} \tag{4}$$

where μ_{h_a} and σ_{h_a} are the normal distribution parameters of EV arrival time in the residential charging pattern; and μ_{h_d} and σ_{h_d} are the normal distribution parameters of EV departure time in the residential charging pattern.

D. Charging Urgency Indicator (CUI) Model

In this paper, a day is divided into T intervals to facilitate the scheduling of EV charging based on the demands across different time intervals. The charging start and end time of each EV can be described as:

$$T_i^a=\left\lceil\frac{t_i^a}{\Delta T}\right\rceil \quad i=1,2,\ldots,N \tag{5}$$

$$T_i^d=\left\lfloor\frac{t_i^d}{\Delta T}\right\rfloor \quad i=1,2,\ldots,N \tag{6}$$

where N is the amount of EVs; i is the index of EV; ΔT is the time interval; t_i^a and t_i^d are the arrival time and the departure time of the i^{th} EV, respectively; T_i^a is the time when the i^{th} EV commences charging, which is rounded up; and T_i^d is the time when the i^{th} EV concludes charging, which is rounded down accordingly.

The CUI is defined to reflect the urgency of EV charging demand [30], which can be expressed as:

$$E_i^{\min}=\left(SOC_i^{\min}-SOC_i^a\right)\cdot Cap_i^{EV} \tag{7}$$

$$CUI_i=\left(T_i^d-T_i^a\right)P_{ch,slow}^{EV}\eta_{ch,i}^{EV}\Delta T-E_i^{\min} \tag{8}$$

where Cap_i^{EV} is the battery capacity of the i^{th} EV; $SOC_i^{\min}$ is the minimum required state of charge (SOC) that EV owners provide before charging in EVCS; $P_{ch,slow}^{EV}$ is the slow charging power; $E_i^{\min}$ is the minimum required energy after the completion of charging; SOC_i^a is the initial SOC for the i^{th} EV; and CUI_i and $\eta_{ch,i}^{EV}$ are the CUI and charging efficiency of the i^{th} EV, respectively.

E. Charging Model Selection

EV owners have the option to select from two charging models, i.e., SC and V2G.

$$P_{ch,i}^{EV}=\begin{cases} P_{ch,fast}^{EV} & CUI_i<0 \\ P_{ch,slow}^{EV} & CUI_i\geq 0 \end{cases} \tag{9}$$

$$P_{dc,i}^{EV,\max}=P_{ch,i}^{EV,\max}=P_{ch,slow}^{EV} \tag{10}$$

where $P_{ch,fast}^{EV}$ is the fast charging power; $P_{ch,i}^{EV}$ is the charging power of the i^{th} EV; and $P_{dc,i}^{EV,\max}$ and $P_{ch,i}^{EV,\max}$ are the maximum discharging and charging power of the i^{th} EV, respectively. The maximum discharging power is equal to the maximum charging power.

In the SC model, EVCS can schedule charging time adaptively according to the charging requirements of the EVs. If $CUI_i<0$, emergency charging is carried out at a power level of $P_{ch,fast}^{EV}$; if $CUI_i\geq 0$, charging is performed at time of relatively low electricity prices through scheduling.

In the V2G model, EVs are considered as ESSs, thus EVCS can assist EV owners in charging at relatively low electricity prices and utilizing the EV battery more efficiently. If $CUI_i<0$, emergency charging is once again executed at a power level of $P_{ch,fast}^{EV}$; if $CUI_i\geq 0$, arbitrage is conducted through scheduled charging and discharging. The charging and discharging power is depicted as shown in (10).

F. Energy Storage Model

DREOs and EVCSs all incorporate ESSs. The energy storage model of DREOs is depicted in (11)-(16), and the energy storage model of the EV is outlined in (17)-(22).

$$E_t^D=E_{t-1}^D+P_{ch,t}^D\Delta T\eta_{ch}^D-P_{dc,t}^D\Delta T/\eta_{dc}^D \tag{11}$$

$$SOC_{\min}\leq E_t^D/E_{*\max}\leq SOC_{\max} \tag{12}$$

$$0\leq P_{ch,t}^D\leq P_{ch}^{\max}S_{ch}^D \tag{13}$$

$$0\leq P_{dc,t}^D\leq P_{dc}^{\max}S_{dc}^D \tag{14}$$

$$S_{ch}^D+S_{dc}^D\leq 1 \tag{15}$$

$$C_t^D=a_D\left(P_{ch,t}^D\eta_{ch}^D+P_{dc,t}^D/\eta_{dc}^D\right)\Delta T \tag{16}$$

$$0\leq P_{ch,i,t}^{EV}\leq P_{ch,i}^{EV,\max}S_{ch,i}^{EV} \tag{17}$$

$$0\leq P_{dc,i,t}^{EV}\leq P_{dc,i}^{EV,\max}S_{dc,i}^{EV} \tag{18}$$

$$S_{ch,i}^{EV}+S_{dc,i}^{EV}\leq 1 \tag{19}$$

$$SOC_{i,t}^{EV}=SOC_{i,t-1}^{EV}+\frac{P_{ch,i,t}^{EV}\eta_{ch,i}^{EV}-P_{dc,i,t}^{EV}/\eta_{dc,i}^{EV}}{Cap_i^{EV}}\Delta T \tag{20}$$

$$SOC_i^a\leq SOC_{i,t}^{EV}\leq SOC_i^{\max} \tag{21}$$

$$SOC_i^{\min}\leq SOC_{i,T_i^d}^{EV}\leq SOC_i^{\max} \tag{22}$$

where E_t^D is the energy state of the ESSs at time t; $E_{*\max}$ is the maximum battery capacity of the ESSs; $P_{ch,t}^D$ and $P_{dc,t}^D$ are the charging and discharging power of the ESSs, respectively; η_{ch}^D and η_{dc}^D are the charging and discharging efficiencies of the ESSs, respectively; $P_{ch}^{\max}$ and $P_{dc}^{\max}$ are the upper bounds of charging and discharging power, respectively; $SOC_{\min}$ and $SOC_{\max}$ are the minimum SOC and maximum SOC, respectively; S_{ch}^D and S_{dc}^D are the charging and discharging indicators, respectively, wherein charging and discharging cannot occur simultaneously; C_t^D is the cost incurred by the ESSs; a_D is the battery degradation parameter; $SOC_i^{\max}$ is the maximum SOC of the i^{th} EV; $SOC_{i,t}^{EV}$ and $SOC_{i,T_i^d}^{EV}$ are the SOCs of the i^{th} EV at time t and T_i^d, respectively; $P_{ch,i,t}^{EV}$ and $P_{dc,i,t}^{EV}$ are the charging and discharging power of the i^{th} EV at time t, respectively; $S_{ch,i}^{EV}$ and $S_{dc,i}^{EV}$ are the charging and discharging indicators of the i^{th} EV, respectively; and $\eta_{dc,i}^{EV}$ is the discharging efficiency of the i^{th} EV.

III. Operation Models

A. Independent Operation Model

When operating independently, DREOs engage in arbitrage via ESSs, storing energy during low electricity price periods and selling it to SO during peak electricity price periods. The profit obtained from the independent operation of the DREOs $F_{in,D}$ is outlined in (23). The power balance constraint is shown in (24). Due to the limited capacity of transmission lines, the network operation constraint is shown in (25).

$$\max F_{in,D}=\sum_{s=1}^{S}\rho_s\sum_{t=1}^{T}\left(\pi_{s,t}^{sale}P_{s,t}^{D,sale}\Delta T-P_{s,t}^{D,buy}\pi_{s,t}^{buy}\Delta T-C_{s,t}^D\right) \tag{23}$$

$$P_{s,t}^D+P_{dc,s,t}^D+P_{s,t}^{D,buy}=P_{s,t}^{D,sale}+P_{ch,s,t}^D \tag{24}$$

$$-G_{\max}\leq P_{s,t}^{D,sale}-P_{s,t}^{D,buy}\leq G_{\max} \tag{25}$$

where ρ_s is the probability of occurrence of scenario s; $P_{s,t}^{D,sale}$ and $P_{s,t}^{D,buy}$ are the power that DREOs sell to and purchase from SO, respectively; $P_{s,t}^D$ is the power generated by distributed renewable energy; $\pi_{s,t}^{buy}$ and $\pi_{s,t}^{sale}$ are the prices of purchasing and selling power from/to SO, respectively; $C_{s,t}^D$ is the cost incurred by the ESSs of scenario s; $P_{ch,s,t}^D$ and $P_{dc,s,t}^D$ are the charging and discharging power of scenario s, respectively; and $G_{\max}$ is the maximum capacity of transmission lines.

EV owners can choose between two charging models, i.e., SC and V2G, as illustrated in Fig. 2. $F_{in1,EV}$ and $F_{in2,EV}$ are the profits obtained from the independent operation of EVCS in the SC model and V2G model described in (26) and (27), respectively. The power balance constraint for the V2G model is shown in (28), with $P_{dc,s,t}^{EV,sum}$ being 0 in the SC model. The network operation constraint for the V2G model is shown in (29), with $P_{s,t}^{EV,sale}$ being 0 in the SC model.

$$\max F_{in1,EV}=\sum_{s=1}^{S}\rho_s\sum_{t=1}^{T}\left(P_{ch,s,t}^{EV,sc}\pi_{s,t}^{EV,1}+P_{ch,s,t}^{EV,fast}\pi_{s,t}^{EV,3}-P_{s,t}^{EV,buy}\pi_{s,t}^{buy}\right)\Delta T \tag{26}$$

$$\max F_{in2,EV}=\sum_{s=1}^{S}\rho_s\sum_{t=1}^{T}\Big(P_{ch,s,t}^{EV,v2g}\pi_{s,t}^{EV,2}+P_{ch,s,t}^{EV,fast}\pi_{s,t}^{EV,3}-P_{s,t}^{EV,buy}\pi_{s,t}^{buy}+P_{s,t}^{EV,sale}\pi_{s,t}^{sale}-P_{dc,s,t}^{EV,sum}\pi_{s,t}^{EV,cop}\Big)\Delta T \tag{27}$$

$$P_{ch,s,t}^{EV,sum}+P_{s,t}^{EV,sale}=P_{s,t}^{EV,buy}+P_{dc,s,t}^{EV,sum} \tag{28}$$

$$-G_{\max}\leq P_{s,t}^{EV,sale}-P_{s,t}^{EV,buy}\leq G_{\max} \tag{29}$$

where $P_{ch,s,t}^{EV,sum}$ and $P_{dc,s,t}^{EV,sum}$ are calculated based on the total charging and discharging power as illustrated in Fig. 2; $P_{ch,s,t}^{EV,sc}$ and $P_{ch,s,t}^{EV,fast}$ are the total charging power for EVs in the SC model and the fast charging model, respectively; $P_{ch,s,t}^{EV,v2g}$ is the actual total power for EVs in the V2G model, which is equal to the total charging power minus the total discharging power; $\pi_{s,t}^{EV,1}$, $\pi_{s,t}^{EV,2}$, and $\pi_{s,t}^{EV,3}$ are the charging prices when EV owners choose the SC model, the V2G model, and the fast charging model, respectively; $\pi^{EV,cop}_{s,t}$ is the discharge compensation price for EVs in the V2G model; and $P^{EV,sale}_{s,t}$ and $P^{EV,buy}_{s,t}$ are the power that EVCSs sell to and buy from SO, respectively.

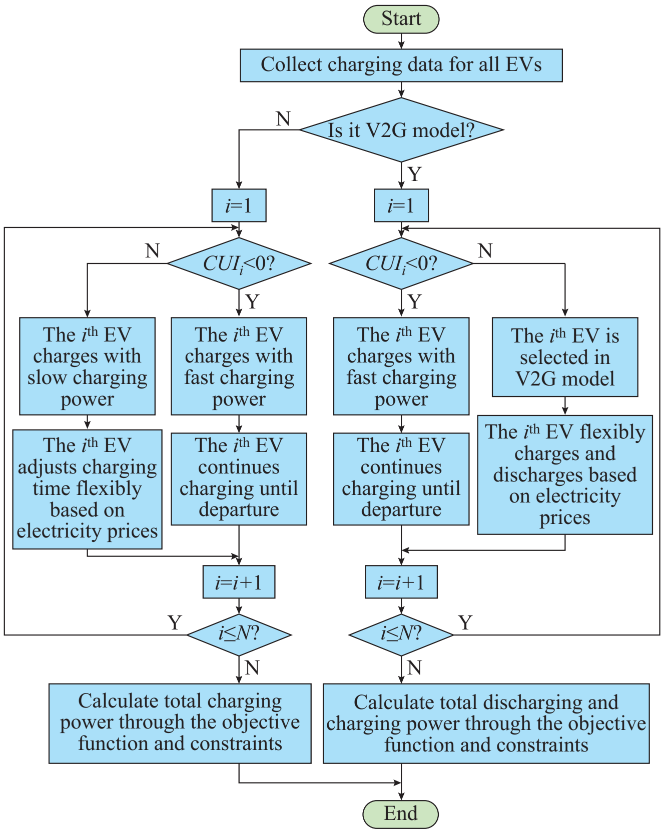

Fig. 2. Flow chart of independent operation in V2G and SC models.

B. Collaborative Operation Model

During collaborative operation, the power balance constraint for V2G model is shown in (30), with $P^{EV,sum}_{dc,s,t}$ being 0 in the SC model. In DREOs, the network operation constraints are shown in (31) and (32). In EVCSs, the network operation constraints for V2G model are shown in (33), with $P^{EV,sale}_{s,t}$ being 0 in the SC model.

$$P^{D}_{s,t}+P^{D}_{dc,s,t}+P^{EV,sum}_{dc,s,t}+P^{EV,buy}_{s,t}+P^{D,buy}_{s,t}=P^{EV,sale}_{s,t}+P^{D,sale}_{s,t}+P^{D}_{ch,s,t}+P^{EV,sum}_{ch,s,t} \tag{30}$$

$$-G_{\max}\le P^{D,sale}_{s,t}-P^{D,buy}_{s,t}\le G_{\max} \tag{31}$$

$$-G_{\max}\le P^{D}_{s,t}+P^{D}_{dc,s,t}+P^{D,buy}_{s,t}-P^{D,sale}_{s,t}-P^{D}_{ch,s,t}\le G_{\max} \tag{32}$$

$$-G_{\max}\le P^{EV,sale}_{s,t}-P^{EV,buy}_{s,t}\le G_{\max} \tag{33}$$

The total profit for collaborative operation in the SC model F_{co1} and the V2G model F_{co2} can be described as:

$$F_{co1}=\sum_{s=1}^{S}\rho_s\sum_{t=1}^{T}\Big[\Big(P^{EV,sale}_{s,t}\pi^{sale}_{s,t}+P^{D,sale}_{s,t}\pi^{sale}_{s,t}-P^{EV,buy}_{s,t}\pi^{buy}_{s,t}-P^{D,buy}_{s,t}\pi^{buy}_{s,t}+P^{EV,sc}_{ch,s,t}\pi^{EV,1}_{s,t}+P^{EV,fast}_{ch,s,t}\pi^{EV,3}_{s,t}\Big)\Delta T-C^{D}_{s,t}\Big] \tag{34}$$

$$F_{co2}=\sum_{s=1}^{S}\rho_s\sum_{t=1}^{T}\Big[\Big(P^{EV,sale}_{s,t}\pi^{sale}_{s,t}+P^{D,sale}_{s,t}\pi^{sale}_{s,t}-P^{EV,buy}_{s,t}\pi^{buy}_{s,t}-P^{D,buy}_{s,t}\cdot\pi^{buy}_{s,t}+P^{EV,v2g}_{ch,s,t}\pi^{EV,2}_{s,t}+P^{EV,fast}_{ch,s,t}\pi^{EV,3}_{s,t}-P^{EV,sum}_{dc,s,t}\pi^{EV,cop}_{s,t}\Big)\Delta T-C^{D}_{s,t}\Big] \tag{35}$$

IV. Proposed Profit Allocation Method

In cooperative games, the Shapley value method is frequently utilized for addressing the allocation of profits among cooperative members. By calculating the marginal contribution of each member, profits are allocated accordingly. The AS method is an improvement over the Shapley value method, enabling faster resolution of profit allocation problems. In [21], the GL-AS method is proposed, thereby achieving a more efficient solution to profit allocation problems. The GL-AS method and the AS method are described as:

$$\begin{cases} F=\max F_{co}\left(x_{co,1},x_{co,2},\dots,x_{co,k}\dots,x_{co,n_{co}}\right)\\ \text{s.t.}\quad \bar{\kappa},k=1,2,\dots,n_{co}\end{cases} \tag{36}$$

where F is the overall profit maximization function for the cooperative alliance; $x_{co,k}$ is the power output of the k^{th} cooperative member; n_{co} is the number of cooperative members; and $\bar{\kappa}$ encompasses all constraint conditions. The profit allocated to the k^{th} cooperative member F_k is calculated by the AS method in (37).

$$F_k=\int_{x^{\min}_{co,k}}^{x^{\max}_{co,k}}\frac{\partial F}{\partial x_{co,k}}\mathrm{d}x_{co,k} \tag{37}$$

where $x^{\min}_{co,k}$ and $x^{\max}_{co,k}$ are the minimum and maximum power outputs of the k^{th} cooperative member, respectively. Divide the power output of the k^{th} member equally into U segments, thereby achieving the discretization of (37). The specific process is described as:

$$\lambda=\frac{x_{co,k}-x^{\min}_{co,k}}{x^{\max}_{co,k}-x^{\min}_{co,k}} \tag{38}$$

$$F_k=\left(x^{\max}_{co,k}-x^{\min}_{co,k}\right)\int_0^1\frac{\partial F\left(x^{\min}_{co,k}+\lambda\left(x^{\max}_{co,k}-x^{\min}_{co,k}\right)\right)}{\partial x_{co,k}}\mathrm{d}\lambda \tag{39}$$

where λ is the auxiliary parameter that comprises U values indexed by $u=1,2,\dots,U$, with each value constrained within the interval $[0,1]$. As the number of segments approaches infinity, the profit from each segment ΔF takes on the following form:

$$\Delta F=F\left(x^{\min}_{co,k}+\lambda_u\left(x^{\max}_{co,k}-x^{\min}_{co,k}\right)\right)-F\left(x^{\min}_{co,k}+\lambda_{u-1}\left(x^{\max}_{co,k}-x^{\min}_{co,k}\right)\right)=\pi_u\Delta x^{u}_{co,k}=\pi_u x_{co,k}\left(\lambda_u-\lambda_{u-1}\right) \tag{40}$$

where λ_u is the u^{th} auxiliary parameter; and π_u is the value of the unknown expression function $\partial F/\partial x_{co,k}$ on the point $x^{u}_{co,k}$. The profit allocated to the k^{th} cooperative member in the discretized solution of the AS method is given by:

$$F_k=\frac{\sum_{t=1}^{T}\sum_{u=1}^{U}\pi_{u,t}\Delta x^{u,t}_{co,k}}{\sum_{k=1}^{n_{co}}\sum_{t=1}^{T}\sum_{u=1}^{U}\pi_{u,t}\Delta x^{u,t}_{co,k}}F \tag{41}$$

where $\pi_{u,t}$ can be calculated in (36), approximately solved using finite difference approximation. Since the output of each member is divided equally, the value of $\Delta x^{u,t}_{co,k}$ is fixed.

Furthermore, it can be observed that (37) is highly consistent with the Gauss-Legendre quadrature formula, thus can be modified as:

$$F_k = \frac{x_{co,k}^{\max} - x_{co,k}^{\min}}{2} \int_{-1}^{1} \frac{\partial F\left(z_k\right)}{\partial x_{co,k}} \mathrm{d}z = \frac{x_{co,k}^{\max} - x_{co,k}^{\min}}{2} \sum_{v=1}^{m} A_v \pi_v\left(z_v\right) \tag{42}$$

$$z_v = \frac{1}{2}\left(z_{k,v}+1\right)\left(x_{co,k}^{\max} - x_{co,k}^{\min}\right) + x_{co,k}^{\min} \quad v = 1, 2, ..., m \tag{43}$$

$$z_k = \frac{1}{2}\left(z+1\right)\left(x_{co,k}^{\max} - x_{co,k}^{\min}\right) + x_{co,k}^{\min} \tag{44}$$

where m is the total number of interpolation points. Interpolation point weight coefficient A_v can be calculated using the Gauss-Legendre quadrature formula and interpolation point $z_{k,v}$.

Due to the profit allocation problem of the cooperative alliance composed of DREOs and EVCSs being highly consistent with cooperative game theory, it is solved using the GL-AS method and AS method. However, during the process of profit allocation, as each member of the cooperative alliance is equipped with ESSs, which may either charge or discharge during each time period, it is found that (36)-(44) do not address the issue of state transformation between charging and discharging of ESSs directly. Meanwhile, P_s^D represents typical scenarios of WP and PV power output, where the power output exhibits volatility across different time intervals. Therefore, the profit allocation cannot be directly solved. Consequently, these cases are discussed and analyzed in this paper.

In the AS method, the constraints on charging and discharging ESSs are modified by using the Big-M method to calculate the profit allocation of ESSs in (45)-(48). The maximum charging and discharging power need to be multiplied by λ_u, so as to ensure that the charging and discharging power is segmented. Meanwhile, it also addresses the non-convex problem during the operation of ESSs.

$$\begin{cases} 0 \le P_{ch,t}^D \le \lambda_u P_{ch}^{\max} \\ 0 \le P_{ch,t}^D \le \lambda_u P_{dc}^{\max} \end{cases} \tag{45}$$

$$\begin{cases} 0 \le P_{ch,t}^D \le M S_{ch}^D \\ 0 \le P_{dc,t}^D \le M S_{dc}^D \end{cases} \tag{46}$$

$$\begin{cases} 0 \le P_{ch,i,t}^{EV} \le \lambda_u P_{ch,i}^{EV,\max} \\ 0 \le P_{dc,i,t}^{EV} \le \lambda_u P_{dc,i}^{EV,\max} \end{cases} \tag{47}$$

$$\begin{cases} 0 \le P_{ch,i,t}^{EV} \le M S_{ch,i}^{EV} \\ 0 \le P_{dc,i,t}^{EV} \le M S_{dc,i}^{EV} \end{cases} \tag{48}$$

where M is considered to be a large number. In the profit allocation of DREOs, DREOs contain distributed renewable energy and ESSs, where $x_{co,k,t}^{\min}$ is 0, and $x_{co,k,t}^{\max}$ is $P_{s,t}^D$ plus the maximum charging power, respectively. The maximum charging power and discharging power are equal in this paper. In the profit allocation of EVCSs, $x_{co,k,t}^{\min}$ equals 0 and $x_{co,k,t}^{\max}$ is the sum of the maximum charging power of all EVs.

In the GL-AS method, after modifying the constraints using the Big-M method, the ESS charging and discharging power constraints are consistent with the general solution form of the GL-AS method, which can be calculated directly. In the profit allocation of EVCSs, the process is the same as that of the AS method.

In the profit allocation of DREOs, since the output power of DREOs varies in each time period, it is necessary to modify the GL-AS method accordingly for each period. The specific process is given as:

$$z_{v,t} = \frac{\left(z_{k,v}+1\right)\left(x_{co,k,t}^{\max} - x_{co,k,t}^{\min}\right)}{2} + x_{co,k,t}^{\min} \tag{49}$$

$$\begin{aligned} F_k = & \sum_{t=1}^{T}\left(\frac{x_{co,k,t}^{\max} - x_{co,k,t}^{\min}}{2} \int_{-1}^{1} \frac{\partial F\left(z_{k,t}\right)}{\partial x_{co,k,t}} \mathrm{d}z\right) = \\ & \sum_{t=1}^{T}\left(\frac{x_{co,k,t}^{\max} - x_{co,k,t}^{\min}}{2} \sum_{v=1}^{m} A_v \pi_{v,t}\left(z_{v,t}\right)\right) \end{aligned} \tag{50}$$

V. Profit Allocation Adjustment Model

In the process of profit allocation, the Shapley value method faces some limitations, notably its failure to consider the factors affecting cooperation. As an improvement to the Shapley value method, the GL-AS method enhances solution efficiency, yet also fails to take into account the factors affecting cooperation.

In this paper, to ensure a more fair profit allocation among cooperative members, several factors affecting cooperation are selected to adjust the profit allocation results. The primary factors identified as impacting profit allocation include RL, PCR, and PGR.

The RL is determined by the S-shaped utility function $\varphi(\cdot)$, with its specific expression provided in Supplementary Material A. Since EVCSs have two charging models, both of which involve energy arbitrage amid electricity price fluctuations, risk preference functions are selected to quantify their risks. In DREOs, ESSs are similar to EVCSs in that they tend to be risk preferring. However, since the power output of distributed renewable energy is non-dispatchable, risk aversion functions are chosen to quantify the associated risks. The RL of the k^{th} cooperative member can be described as:

$$RL_k = \frac{\varphi\left(x_{co,k}\right)}{\sum_{k=1}^{n_{co}} \varphi\left(x_{co,k}\right)} \tag{51}$$

The GL-AS method allocates results based only on the marginal contributions of each cooperative member (independent operation profits plus the excess profit (EP) generated after collaborative operation), without taking into account the proportion of EP that each member gains after collaborative operation. The PCR of the k^{th} cooperative member can be calculated as:

$$PCR_k = \frac{F_{co,k} - F_{in,k}}{\sum_{k=1}^{n_{co}}\left(F_{co,k} - F_{in,k}\right)} \tag{52}$$

where $F_{in,k}$ and $F_{co,k}$ are the profits of the k^{th} member before and after cooperation, respectively.

PGR reflects the profit growth situation before and after cooperation, which will affect the cooperative willingness of each member. Therefore, to promote the stable development of the cooperative alliance, the impact of PGR cannot be ignored. The PGR of the k^{th} cooperative member can be described as:

$$PGR_k = \frac{\left(F_{co,k} - F_{in,k}\right) / F_{in,k}}{\sum_{k=1}^{n_{co}} \left(F_{co,k} - F_{in,k}\right) / F_{in,k}} \tag{53}$$

The impact of these factors affecting cooperation is not to be ignored. Consequently, the subjective and objective evaluations within the TFCE method are utilized for the fair profit allocation. This method is capable of effectively managing the uncertainties and ambiguities inherent in multiple evaluation indicators, thereby ensuring the fairness and rationality of the profit allocation scheme. With the contributions and corresponding cooperative impacts of each member calculated, profits are allocated in a manner that promotes the long-term stable development of cooperative relationships.

A. TFN-AHP Method

For most individuals, accurately addressing complex and chaotic decision-making challenges is perceived as a significant difficulty. This is attributed to the tendency to rely on vague judgments unconsciously during the process of making choices and judgments. The triangular fuzzy number model is highlighted as particularly crucial, as it employs three elements to depict the accuracy of a judgment, thereby thoroughly accommodating the characteristic fuzziness in human judgment. By quantifying uncertainties within decision-making, a deeper understanding and analysis of decision-making issues are facilitated, allowing for a more objective evaluation of various potential outcomes. In this paper, there are V evaluation items (equal to the number of scenarios) and R evaluation indicators. The fuzzy judgment matrix is described as $\boldsymbol{A} = \left(\boldsymbol{a}_{rj}\right)_{R\times R}$, where $\boldsymbol{a}_{rj} = \left[l_{rj}, m_{rj}, u_{rj}\right]$, and $\boldsymbol{a}_{jr} = \boldsymbol{a}_{rj}^{-1}$.

$$\boldsymbol{a}_{rj} = \frac{1}{H} \otimes \left(a_{rj}^1 + a_{rj}^2 + ... + a_{rj}^h + ... + a_{rj}^H\right) \quad h = 1, 2, ..., H \tag{54}$$

where m_{rj} is the expert judgment on the relative importance of two indicators; l_{rj} and u_{rj} are the lower and upper bounds of the fuzzy evaluation interval, respectively; H is the number of experts participating in the evaluation; and a_{rj}^h is the triangular fuzzy number given by the h^{th} expert during the evaluation process. The fuzzy weight of the r^{th} evaluation indicator W_r is calculated as:

$$W_r = \frac{\sum_{j=1}^{R} a_{rj}}{\sum_{r=1}^{R}\sum_{j=1}^{R} a_{rj}} = \left(\frac{\sum_{j=1}^{R} a_{rj}^l}{\sum_{r=1}^{R}\sum_{j=1}^{R} a_{rj}^u}, \frac{\sum_{j=1}^{R} a_{rj}^m}{\sum_{r=1}^{R}\sum_{j=1}^{R} a_{rj}^m}, \frac{\sum_{j=1}^{R} a_{rj}^u}{\sum_{r=1}^{R}\sum_{j=1}^{R} a_{rj}^l}\right) \quad r = 1, 2, ..., R \tag{55}$$

To calculate the non-fuzzy weight, it is necessary to make pairwise comparisons of the fuzzy weights. The comparison probability matrix $\boldsymbol{B}\left(W_r \geq W_j\right) = \left(b_{rj}\right)_{R\times R}$ is depicted as:

$$b_{rj} = \begin{cases} 1 & m_r \geq m_j \\ W_{rj} & m_r \leq m_j, u_r \geq u_j \\ 0 & l_j \geq u_r \end{cases} \tag{56}$$

where W_{rj} is the value of $\left(l_j - u_r\right) / \left(m_r - u_r - m_j + l_j\right)$. Indicated by the possibility matrix $\boldsymbol{B}$, the comprehensive importance of the r^{th} factor relative to other factors O_r is given by:

$$O_r = \min b_{rj} \quad j = 1, 2, \ldots, R, j \neq r \tag{57}$$

The weight vector $\left[O_1, O_2, \ldots, O_R\right]$ is obtained based on (57). Therefore, the subjective weight of the r^{th} indicator ω_{ar} can be described as:

$$\omega_{ar} = \frac{O_r}{\sum_{r=1}^{R} O_r} \tag{58}$$

B. EW Method

The EW method is identified as an objective weighting method based on the principle of information entropy, utilized for determining the weights of various evaluation indicators. By analyzing the entropy values among indicators, differences and significance among indicators are effectively identified, thereby providing a quantified basis for decision-making.

Calculating the objective weight of EW ω_{qr} requires obtaining the objective evaluation coefficient matrix $\boldsymbol{Q} = \left(q_{vr}\right)_{V\times R}$ through objective calculations. Subsequently, the evaluation coefficient matrix is to be subjected to normalization as:

$$d_{vr} = \frac{q_{vr}}{\sum_{v=1}^{V} q_{vr}} \quad v = 1, 2, ..., V, r = 1, 2, ..., R \tag{59}$$

where d_{vr} is the element of matrix $\boldsymbol{D}$ after normalization, whose dimension is $V \times R$. The entropy value e_r and redundancy degree h_r of the r^{th} indicator are to be calculated through (60) and (61).

$$e_r = -\ln R \cdot \sum_{v=1}^{V} d_{vr} \ln d_{vr} \tag{60}$$

$$h_r = 1 - e_r \tag{61}$$

The r^{th} objective weight ω_{qr} according to the entropy method can be calculated as:

$$\omega_{qr} = \frac{h_r}{\sum_{r=1}^{R} h_r} \tag{62}$$

C. Comprehensive Weight

In this paper, by adopting the principle of minimum discrimination information [31], a combination of subjective and objective weights is achieved, thereby allowing for the derivation of a comprehensive weight ω_r for each evaluation indicator in (63).

$$\begin{cases} \min \sum_{r=1}^{R} \left(\omega_r \ln \frac{\omega_r}{\omega_{ar}} + \omega_r \ln \frac{\omega_r}{\omega_{qr}}\right) \\ \text{s.t.} \ \sum_{r=1}^{R} \omega_r = 1 \quad \omega_r \geq 0, r = 1, 2, ..., R \end{cases} \tag{63}$$

The comprehensive weight for the r^{th} evaluation indicator can be calculated as:

$$\omega_r = \frac{\sqrt{\omega_{ar}\omega_{qr}}}{\sum_{r=1}^{R} \sqrt{\omega_{ar}\omega_{qr}}} \tag{64}$$

Therefore, the revised profit allocated to the k^{th} member F_k^* can be described as:

$$F_k^* = F_k + F\left(\sum_{r=1}^{R}\omega_r\omega_{r,k} - \frac{1}{n_{co}}\right) \tag{65}$$

VI. Case Studies

In this paper, DREOs are divided into two categories: DREO1 (WP and ESSs) and DREO2 (PV and ESSs). EVCSs are divided into two categories: EVCS1 (public charging pattern) and EVCS2 (residential charging pattern), each with 50 EVs. Five typical scenarios of WP and PV power outputs are selected, with the original scenario dataset sourced from real power output data in Guangdong Province, China. A day is divided into 96 intervals, with each interval spanning 15 min. The travelling data for EVs in EVCS1 and EVCS2 are displayed in Fig. 3, with specific parameters as described in [32]. The probability density function (PDF) curves in Fig. 3 illustrate the distribution of travel data for EV owners at EVCS1 and EVCS2. The ESS data for DREO1 and DREO2 are presented in Table I. The charging data for EVs are presented in Table II. The charging and discharging efficiency is 0.9. The electricity price data are obtained by random sampling from actual PJM market prices. The charging prices in SC model and V2G model are \$0.18. The charging price in fast charging model is \$0.20. The proposed model is constructed using MATLAB/YALMIP and optimized using the CPLEX solver.

A. SC Model

The results of profit allocation in the SC model are shown in Table III. Compared with the total profit from independent operation, the total profit from collaborative operation has an increase of \$145.58, with an overall PGR of 38.10%. During the collaboration operation between DREOs and EVCSs, the profits of all cooperative members increase significantly.

The charging power of EVCSs operating independently and collaboratively in the SC model is displayed in Fig. 4, where the legend "In" represents independent operation, and "Co" represents collaborative operation. These definitions are consistent across the legends of other figures. The selling/purchasing power to/from the SO during independent and collaborative operation in the SC model is displayed in Fig. 5. Compared with EVCS1, EVCS2 operates in a home charging pattern where the electricity purchasing prices are relatively low during the charging periods, thereby resulting in relatively high profit. During the collaborative operation, DREOs can supply power to EVCSs. Since EVCS1 operates in a public charging pattern where the electricity selling prices are relatively high during the charging periods, the increase of profit from the collaborative operation is larger. Compared with DREO2, DREO1 gains more profit due to its continuous power supply to EVCSs.

The weights of profit allocation of each cooperative member in the SC model are displayed in Fig. 6. The AS method, as an extension of the Shapley value method, has allocation results generally close to the Shapley value method. The GL-AS method has higher precision compared with the traditional discretization method.

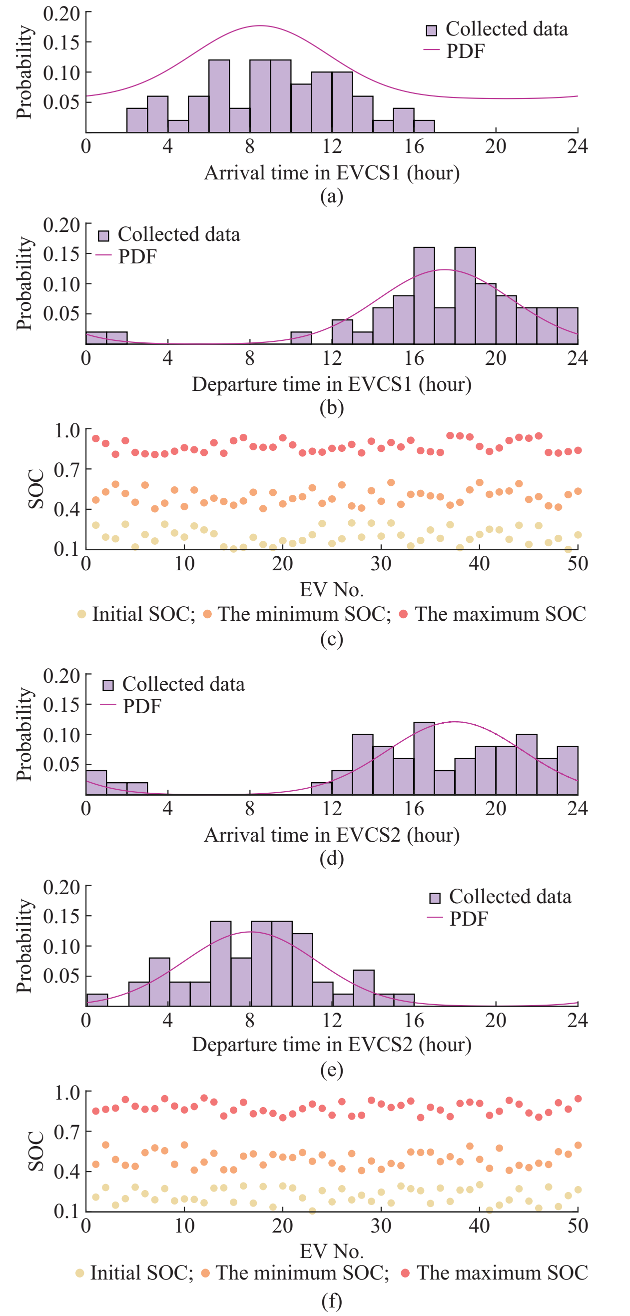

Fig. 3. Travelling data for EVs in EVCS1 and EVCS2. (a) Arrival time of 50 EVs in EVCS1. (b) Departure time of 50 EVs in EVCS1. (c) SOC of 50 EVs in EVCS1. (d) Arrival time of 50 EVs in EVCS2. (e) Departure time of 50 EVs in EVCS2. (f) SOC of 50 EVs in EVCS2.

TABLE I
ESS Data for DREO1 and DREO2

DREO	$E_{\max}$ (kWh)	$P_{ch}^{\max}$ (kW)	$P_{dc}^{\max}$ (kW)
DREO1	100	30.0	30.0
DREO2	125	37.5	37.5

TABLE II
Charging Data for EVs

EVCS	Cap_{EV} (kWh)	$P_{ch,slow}^{EV}$ (kW)	$P_{ch,fast}^{EV}$ (kW)
EVCS1	40	10	15
EVCS2	40	10	15

TABLE III
RESULTS OF PROFIT ALLOCATION IN SC MODEL

Method	Profit ($)				
	EVCS1	EVCS2	DREO1	DREO2	Total
F_{in}	121.86	156.66	53.05	50.57	382.14
Shapley	177.17	194.52	83.06	72.97	527.72
AS	175.46	193.29	84.28	74.69	527.72
GL-AS	176.40	193.89	83.78	73.65	527.72
EP	54.54	37.23	30.73	23.08	145.58

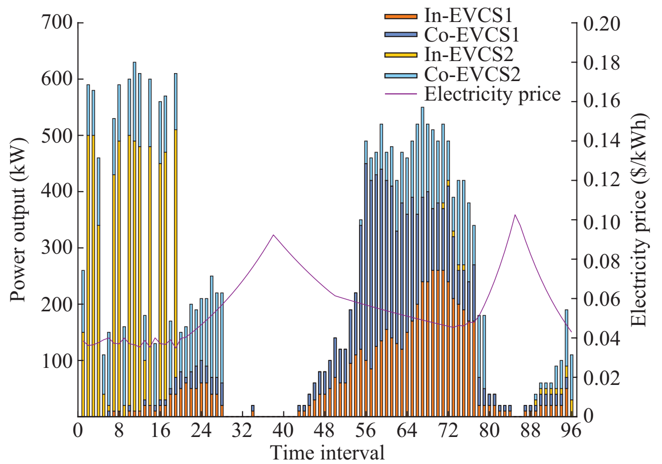

Fig. 4. Charging power of EVCSs operating independently and collaboratively in SC model.

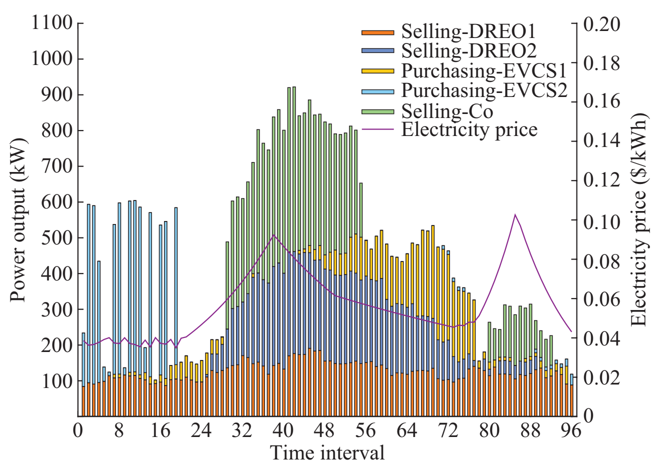

Fig. 5. Selling/purchasing power to/from SO during independent and collaborative operations in SC model.

The weights of cooperative risk factors in the SC model such as PCR, PGR, and RL are comprehensively assessed and displayed in Fig. 7, through the integration of the TFN-AHP and EW methods. Modifications to profit allocation, based on these weights, lead to the final results of profit allocation results presented in Table IV. By replacing the existing assumption of equal weights for the factors that influence cooperation, it is evident that profit allocation becomes more fair. Due to the relatively low proportion of profit allocation weight of EVCS2 compared with the average weight, the profit allocation weights of other collaborating members are higher than the average weight. As a result, part of the profit obtained by the EVCS2 is compensated to other cooperative members. The final profit allocation is larger than what each member would earn when operating independently, which ensures incentive compatibility and individual rationality.

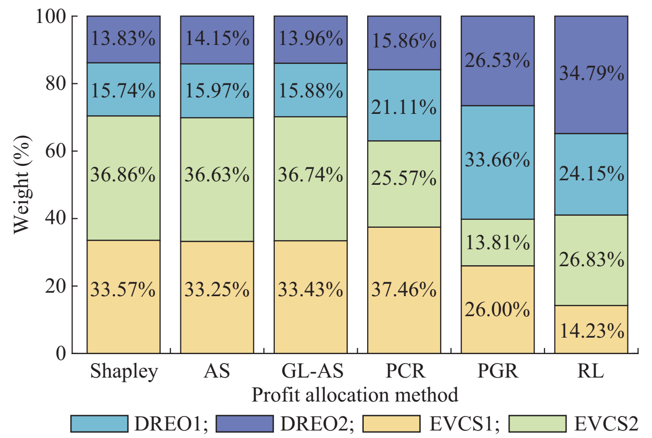

Fig. 6. Weights of profit allocation of each cooperative member in SC model.

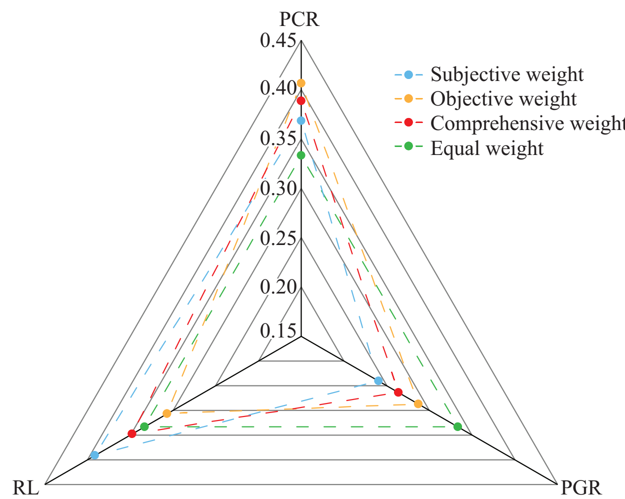

Fig. 7. Weights of cooperative risk factors in SC model.

TABLE IV
FINAL RESULTS OF PROFIT ALLOCATION

Model	Profit ($)				
	EVCS1	EVCS2	DREO1	DREO2	Total
SC	183.57	182.84	86.29	75.02	527.72
V2G	188.13	188.04	95.77	76.32	548.26

B. V2G Model

The results of profit allocation in the V2G model are shown in Table V. The weights of profit allocation of each cooperative member in the V2G model are shown in Fig. 8, the weights of cooperative risk factors in the V2G model are displayed in Fig. 9, the charging and discharging power of EVCS1 and EVCS2 operating independently and collaboratively in the V2G model are shown in Fig. 10 and Fig. 11, and the selling/purchasing power to/from the SO during independent and collaborative operation in the V2G model is displayed in Fig. 12. Compared with the total profit from the independent operation of EVCSs in the SC model, the profit in the V2G model increases significantly. The reason is that in the V2G model, EVs serve as ESSs, enabling them to store power during periods of relatively low electricity purchasing prices, and discharge to provide power when the electricity purchasing prices are relatively high, thereby significantly reducing the charging costs for EVCSs. During collaborative operation, EVs can store power provided by DREOs when electricity purchasing prices are relatively low and discharge power when electricity purchasing prices are relatively high, thereby achieving higher profit growth. Since the comprehensive weights of EVCS2 is relatively low than the average weight, part of the profit earned by EVCS2 is compensated to other cooperative members. The final allocation results are displayed in Table IV.

TABLE V
RESULTS OF PROFIT ALLOCATION IN V2G MODEL

Method	Profit ($)				
	EVCS1	EVCS2	DREO1	DREO2	Total
F_{in}	127.77	163.28	53.05	50.57	394.67
Shapley	185.25	203.19	85.98	73.84	548.26
AS	183.32	201.88	86.72	76.34	548.26
GL-AS	184.05	202.41	86.72	75.08	548.26
EP	56.28	39.13	33.67	24.51	153.59

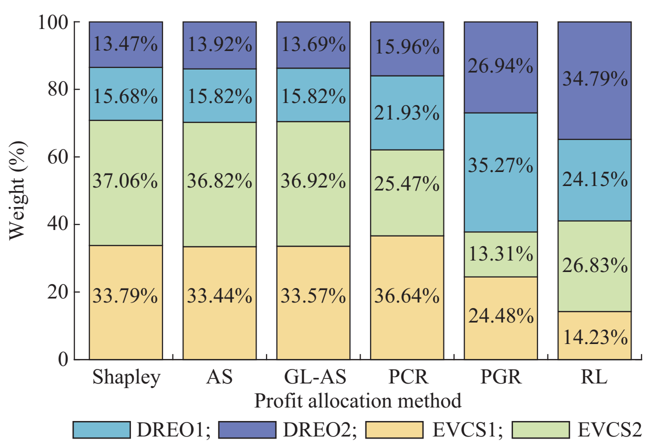

Fig. 8. Weights of profit allocation of each cooperative member in V2G model.

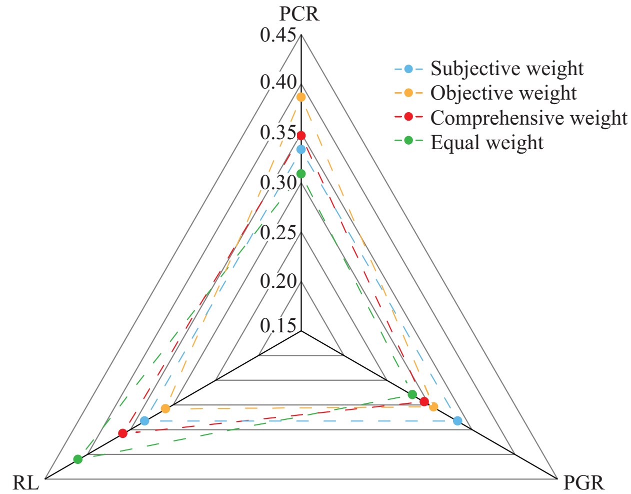

Fig. 9. Weights of cooperative risk factors in V2G model.

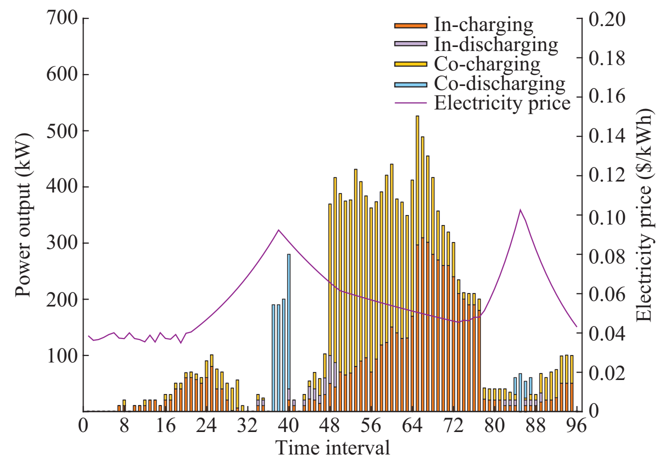

Fig. 10. Charging and discharging power of EVCS1 operating independently and collaboratively in V2G model.

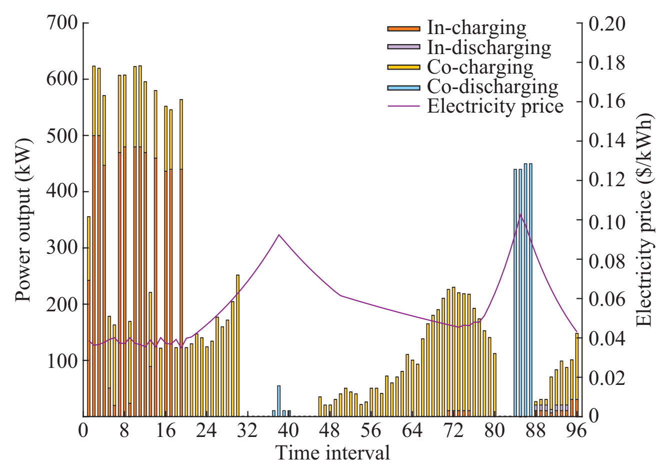

Fig. 11. Charging and discharging power of EVCS2 operating independently and collaboratively in V2G model.

C. Comparison of Calculation Speed

The calculation number of each profit allocation method is shown in Fig. 13. The results calculated by the GL-AS method and the AS method are almost the same. Since the AS method requires selecting at least 30 interpolation points, while the GL-AS method only needs 3 points, the calculation speed of the GL-AS method is about 10 times that of the AS method. In this paper, there are a total of four cooperative members.

Consequently, the Shapley value method requires 16 optimization calculations, the AS method requires 120 optimization calculations, and the GL-AS method only requires 12 optimization calculations. As the number of cooperative members increases, the differences become even more pronounced, thereby ensuring the efficiency of profit allocation calculations.

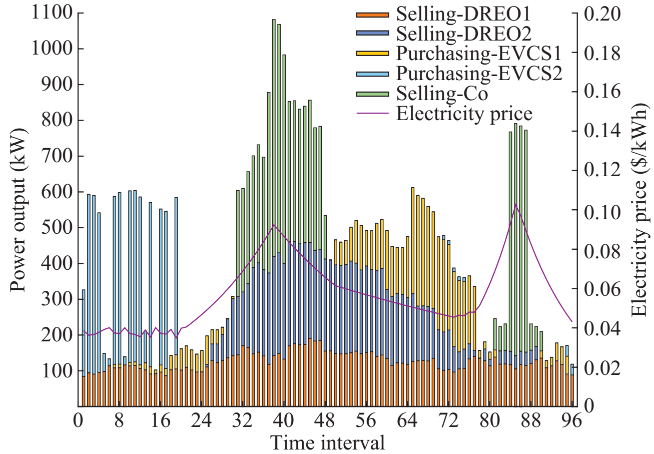

Fig. 12. Selling/purchasing power to/from SO during independent and collaborative operation in V2G model.

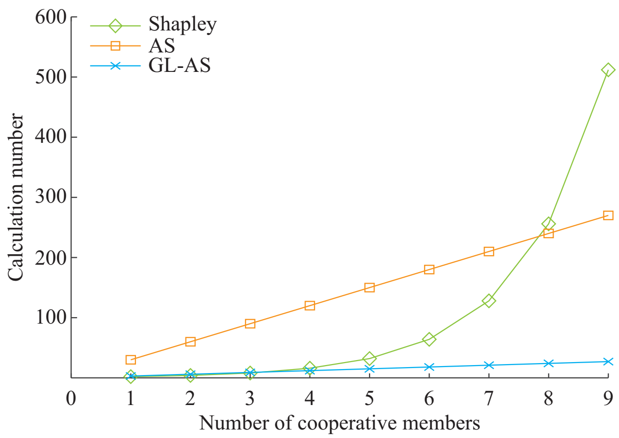

Fig. 13. Calculation number of each profit allocation method.

VII. Conclusion

This paper proposes a profit allocation method for the collaborative operation of DREOs and EVCSs. Firstly, a collaborative operation model is established for DREOs and EVCSs. In the SC model, the collaborative operation increases profit by 38.10% compared with independent operation, and by 38.92% in the V2G model. Secondly, the GL-AS method solves the profit allocation problem 10 times faster than the AS method. Additionally, issues related to ESS switching between charging and discharging in any time interval and the time-varying problem of renewable energy power output in the GL-AS method are addressed, enabling broader application in power systems. Finally, the TFCE method is used to evaluate the weight of factors influencing cooperation, achieving fairness in profit allocation compared with the equal weight used in traditional methods.

References

[1] Y. Wang, J. He, and W. Chen, “Distributed solar photovoltaic development potential and a roadmap at the city level in China,” *Renewable and Sustainable Energy Reviews*, vol. 141, p. 110772, May 2021.

[2] J. Leithon, S. Werner, and V. Koivunen, “Cost-aware renewable energy management: centralized vs. distributed generation,” *Renewable Energy*, vol. 147, pp. 1164-1179, Mar. 2020.

[3] A. Angelus, “Distributed renewable power generation and implications for capacity investment and electricity prices,” *Production and Operations Management*, vol. 30, pp. 4614-4634, Dec. 2021.

[4] A. König, L. Nicoletti, D. Schröder *et al.*, “An overview of parameter and cost for battery electric vehicles,” *World Electric Vehicle Journal*, vol. 12, p. 21, Feb. 2021.

[5] N. Goetzel and M. Hasanuzzaman, “An empirical analysis of electric vehicle cost trends: a case study in germany,” *Research in Transportation Business & Management*, vol. 43, p. 100825, Jun. 2022.

[6] W. Kempton and J. Tomić, “Vehicle-to-grid power fundamentals: calculating capacity and net revenue,” *Journal of Power Sources*, vol. 144, pp. 268-279, Jun. 2005.

[7] I. A. Nienhueser and Y. Qiu, “Economic and environmental impacts of providing renewable energy for electric vehicle charging – a choice experiment study,” *Applied Energy*, vol. 180, pp. 256-268, Oct. 2016.

[8] L. Luo, Z. Wu, W. Gu *et al.*, “Coordinated allocation of distributed generation resources and electric vehicle charging stations in distribution systems with vehicle-to-grid interaction,” *Energy*, vol. 192, p. 116631, Feb. 2020.

[9] S.-W. Park, K.-S. Cho, G. Hoefter *et al.*, “Electric vehicle charging management using location-based incentives for reducing renewable energy curtailment considering the distribution system,” *Applied Energy*, vol. 305, p. 117680, Jan. 2022.

[10] J. Liu and C. Zhong, “An economic evaluation of the coordination between electric vehicle storage and distributed renewable energy,” *Energy*, vol. 186, p. 115821, Nov. 2019.

[11] Y. Meng, G. Ma, Y. Yao *et al.*, “Nash bargaining based integrated energy agent optimal operation strategy considering negotiation pricing for tradable green certificate,” *Applied Energy*, vol. 356, p. 122427, Feb. 2024.

[12] Z. Lu, J. Wang, M. Shahidehpour *et al.*, “Cooperative operation of distributed energy resources and thermal power plant with a carbon-capture-utilization-and-storage system,” *IEEE Transactions on Power Systems*, vol. 39, no. 1, pp. 1850-1866, Jan. 2023.

[13] T. Ma, W. Pei, W. Deng *et al.*, “A nash bargaining-based cooperative planning and operation method for wind-hydrogen-heat multi-agent energy system,” *Energy*, vol. 239, p. 122435, Jan. 2022.

[14] Y. Wu, C. Liu, Z. Lin *et al.*, “Vickrey-Clark-Groves-based method for eradicating deceptive behaviors in demand response transactions,” *Journal of Modern Power Systems and Clean Energy*, vol. 12, no. 4, pp. 1260-1271, Jul. 2024.

[15] M. Jiang, Q. Guo, H. Sun *et al.*, “Leverage reactive power ancillary service under high penetration of renewable energies: an incentive-compatible obligation-based market mechanism,” *IEEE Transactions on Power Systems*, vol. 37, no. 4, pp. 2919-2933, Jul. 2021.

[16] J. Wang, H. Zhong, Z. Yang *et al.*, “Incentive mechanism for clearing energy and reserve markets in multi-area power systems,” *IEEE Transactions on Sustainable Energy*, vol. 11, pp. 2470-2482, Oct. 2019.

[17] Z. Zhang, Y. Huang, Z. Chen *et al.*, “Integrated demand response for microgrids with incentive compatible bidding mechanism,” *IEEE Transactions on Industry Applications*, vol. 59, pp. 118-127, Feb. 2022.

[18] J. Xie, L. Zhang, X. Chen *et al.*, “Incremental benefit allocation for joint operation of multi-stakeholder wind-PV-hydro complementary generation system with cascade hydro-power: an Aumann-Shapley value method,” *IEEE Access*, vol. 8, pp. 68668-68681, Apr. 2020.

[19] E. Faria, L. A. Barroso, R. Kelman *et al.*, “Allocation of firm-energy rights among hydro plants: an Aumann-Shapley approach,” *IEEE Transactions on Power Systems*, vol. 24, no. 2, pp. 541-551, May 2009.

[20] R. Xie and Y. Chen, “Real-time bidding strategy of energy storage in an energy market with carbon emission allocation based on Aumann-Shapley prices,” *IEEE Transactions on Energy Markets, Policy and Regulation*, vol. 2, no. 3, pp. 350-367, Sept. 2024.

[21] L. Zhao, Y. Xue, H. Sun *et al.*, “Benefit allocation for combined heat and power dispatch considering mutual trust,” *Applied Energy*, vol. 345, p. 121279, Sept. 2023.

[22] J. Gao, F. Gao, Y. Yang *et al.*, “Configuration optimization and benefit allocation model of multi-park integrated energy systems considering electric vehicle charging station to assist services of shared energy storage power station,” *Journal of Cleaner Production*, vol. 336, p. 130381, Feb. 2022.

[23] X. Ma, S. Yu, S. Zhu *et al.*, “Profit allocation to virtual power plant members based on improved multifactor Shapley value method,” *Transactions of China Electrotechnical Society*, vol. 35, pp. 585-595, Dec. 2020.

[24] Q. Zheng, H.-M. Lyu, A. Zhou *et al.*, “Risk assessment of geohazards along cheng-kun railway using fuzzy AHP incorporated into GIS,” *Geomatics, Natural Hazards and Risk*, vol. 12, pp. 1508-1531, Jun.

2021.

[25] S. Cai, J. Fan, and W. Yang, “Flooding risk assessment and analysis based on gis and the TFN-AHP method: a case study of Chongqing, China,” *Atmosphere*, vol. 12, p. 623, May 2021.

[26] Z. Luo, J. Zhou, L. Zheng *et al.*, “A TFN-ANP based approach to evaluate virtual research center comprehensive performance,” *Expert Systems with Applications*, vol. 37, pp. 8379-8386, Dec. 2010.

[27] P. Linares, “Multiple criteria decision making and risk analysis as risk management tools for power systems planning,” *IEEE Transactions on Power Systems*, vol. 17, no. 3, pp. 895-900, Aug. 2002.

[28] L. Ávila, M. R. Mine, E. Kaviski *et al.*, “Complementarity modeling of monthly streamflow and wind speed regimes based on a copula-entropy approach: a Brazilian case study,” *Applied Energy*, vol. 259, p. 114127, Feb. 2020.

[29] T. M. Ghazal, “Performances of *k*-means clustering algorithm with different distance metrics,” *Intelligent Automation & Soft Computing*, vol. 30, pp. 735-742, May 2021.

[30] K. Zhou, L. Cheng, L. Wen *et al.*, “A coordinated charging scheduling method for electric vehicles considering different charging demands,” *Energy*, vol. 213, p. 118882, Dec. 2020.

[31] G. P. Karev, “Principle of minimum discrimination information and replica dynamics,” *Entropy*, vol. 12, pp. 1673-1695, Jun. 2010.

[32] A. Schuller, C. M. Flath, and S. Gottwalt, “Quantifying load flexibility of electric vehicles for renewable energy integration,” *Applied Energy*, vol. 151, pp. 335-344, Aug. 2015.

Wei Zha is currently pursuing the M.S. degree at Tsinghua University, Beijing, China. His research interests include electricity market and power system operation.

Haiwang Zhong received the B.S. and Ph.D. degrees in electrical engineering from Tsinghua University, Beijing, China, in 2008 and 2013, respectively. He is currently an Associate Professor with the Department of Electrical Engineering, Tsinghua University, Beijing, China. He is also the Director of the Energy Internet Trading and Operation Research Department, Sichuan Energy Internet Research Institute, Tsinghua University. His research interests include power system operation and optimization, and electricity market.

Yinyan Liu received the B.S. degree from North China Electric Power University, Beijing, China, the M.S. degree from Tsinghua University, Beijing, China, and the Ph.D. degree from the University of Sydney, Sydney, Australia, in 2011, 2018, and 2022, respectively. She is currently a Postdoctoral Research Associate with the School of Photovoltaic and Renewable Energy Engineering, University of New South Wales, Sydney, Australia. Her research interests include demand response for decarbonization and decentralization, operation and maintenance of distributed energy resources, and application of artificial intelligence in smart cities and smart grids.